Real and reciprocal space structural correlations contributing to the first sharp diffraction peak in silica glass

T. Uchino,[1,2] J. D. Harrop,[3] S. N. Taraskin,[3] and S. R. Elliott[3]
[1]*Department of Chemistry, Kobe University, Nada-ku, Kobe 657-8501, Japan*
[2]*PRESTO, Japan Science and Technology Agency, Honcho Kawaguchi, Saitama 332-0012, Japan*
[3]*Department of Chemistry, University of Cambridge, Cambridge CB2 1EW, United Kingdom*
(Received 10 December 2003; revised manuscript received 6 October 2004; published 12 January 2005)

We have applied a "real-reciprocal space analysis," using the continuous wavelet transform technique, to the experimental neutron and x-ray structure factors of silica glass to elucidate a correlation between the "first sharp diffraction peak (FSDP)" in reciprocal space and the corresponding length scale in real space. The present analysis allows us to obtain compelling evidence that the dominant interatomic distance linked to the FSDP in silica glass is ~ 5 Å, although longer distances are also important, making an exponentially decreasing contribution. Further analysis using molecular-dynamics simulations demonstrates that the interatomic spatial correlations at $r \sim 5$ Å are associated with a couple of local "pseudo-Bragg" planes having an interlayer separation of ~ 4 Å, accounting for the origin of structural ordering on the medium-range length scale in silica glass.

DOI: 10.1103/PhysRevB.71.014202 PACS number(s): 61.43.Fs, 61.10.Eq, 61.12.Ex

I. INTRODUCTION

The nature of order and disorder on the medium-range length scale (~ 5 to ~ 10 Å) in glasses and liquids has long been debated.[1–5] X-ray and neutron diffraction are commonly used experimental techniques to get information about the atomic arrangements of such noncrystalline materials, not only on a short-range but also on a medium-range length scale. The diffraction data are collected as a function of Q ($=4\pi \sin\theta/\lambda$, where λ is the wavelength of the incident radiation and 2θ the scattering angle) to obtain the structure factor, $S(Q)$, of the corresponding materials. Then the r-space correlations can be obtained by the Fourier transform of $S(Q)$, i.e., a decomposition of the $S(Q)$ function into sine waves of constant amplitude. Thus Fourier transformation is an ideal method to analyze diffraction components that are delocalized over the observed Q range, corresponding to relatively sharp features in r space (e.g., first- and second-neighbor shells of atoms in the structure). However, for components that are localized in limited regions in Q space, such as the anomalous but ubiquitous sharp feature called the "first sharp diffraction peak" (FSDP) seen in $S(Q)$ of many different types of noncrystalline materials,[2] Fourier analysis results in rather delocalized features in r space, conveying little information about the interatomic correlations involved. For this reason, the precise structural origin of FSDP still remains to be solved, although it is believed that the FSDP gives a clue to the extent of medium-range order in glassy and amorphous solids.[6–9]

To circumvent the above problem, we here employ an alternative approach, i.e., a "time-frequency" analysis using the continuous wavelet transform,[10–13] to analyze the observed $S(Q)$ functions. Recently, it has been recognized,[10,12] that the wavelet transform has considerable potential as a tool to investigate locality both in Q and r space (or equivalently in both time and frequency domains). Instead of being based on sinusoidal functions, the method is based on wavelet functions, which are localized in time as well as frequency. That is, the input function is expanded in terms of oscillations of these localized functions in both time and frequency domains simultaneously. Thus the wavelet method should be ideally suited for an analysis of the FSDP, both in terms of Q and r space.

The last decade has witnessed an explosion of applications of wavelets in mathematics and physics to study the temporal and localized behavior of oscillatory signals.[10–13] Previously, Ding *et al.*[14] applied the wavelet method to a structural analysis of diffraction data for silica glass, but the wavelet function that they used was the so-called "Mexican hat" wavelet,[10,11] which is unsuited for the analysis of highly frequency- and amplitude-modulated signals, such as $S(Q)$ for glassy materials.[15] Recently, we[15] have developed a "tunable" complex wavelet function based on the continuous wavelet transform (CWT),[13] which is well suited, as compared with the existing "Mexican hat" wavelet or the Morlet wavelet,[16] to the analysis of one-dimensional signals whose frequency components are rapidly changing in frequency as well as in amplitude. In this work, we have applied this wavelet function[15] to an analysis of the reduced structure factor $Q[S(|Q|)-1]$ for silica glass measured by neutron and high-energy x-ray diffraction techniques. Previous diffraction measurements on silica glass have revealed that the position of the FSDP lies at around 1.5 Å^{-1}, which implies structural correlations in the distance range ~ 3 to ~ 10 Å.[2,7,17] The present wavelet analysis sheds new light on the connection between the FSDP and the corresponding r-space correlations, showing the dominant interatomic distances linked to the FSDP in silica glass.

II. NUMERICAL TECHNIQUES

We have calculated the instantaneous amplitude of the CWT of $Q[S(|Q|)-1]$ using neutron[18] and high-energy

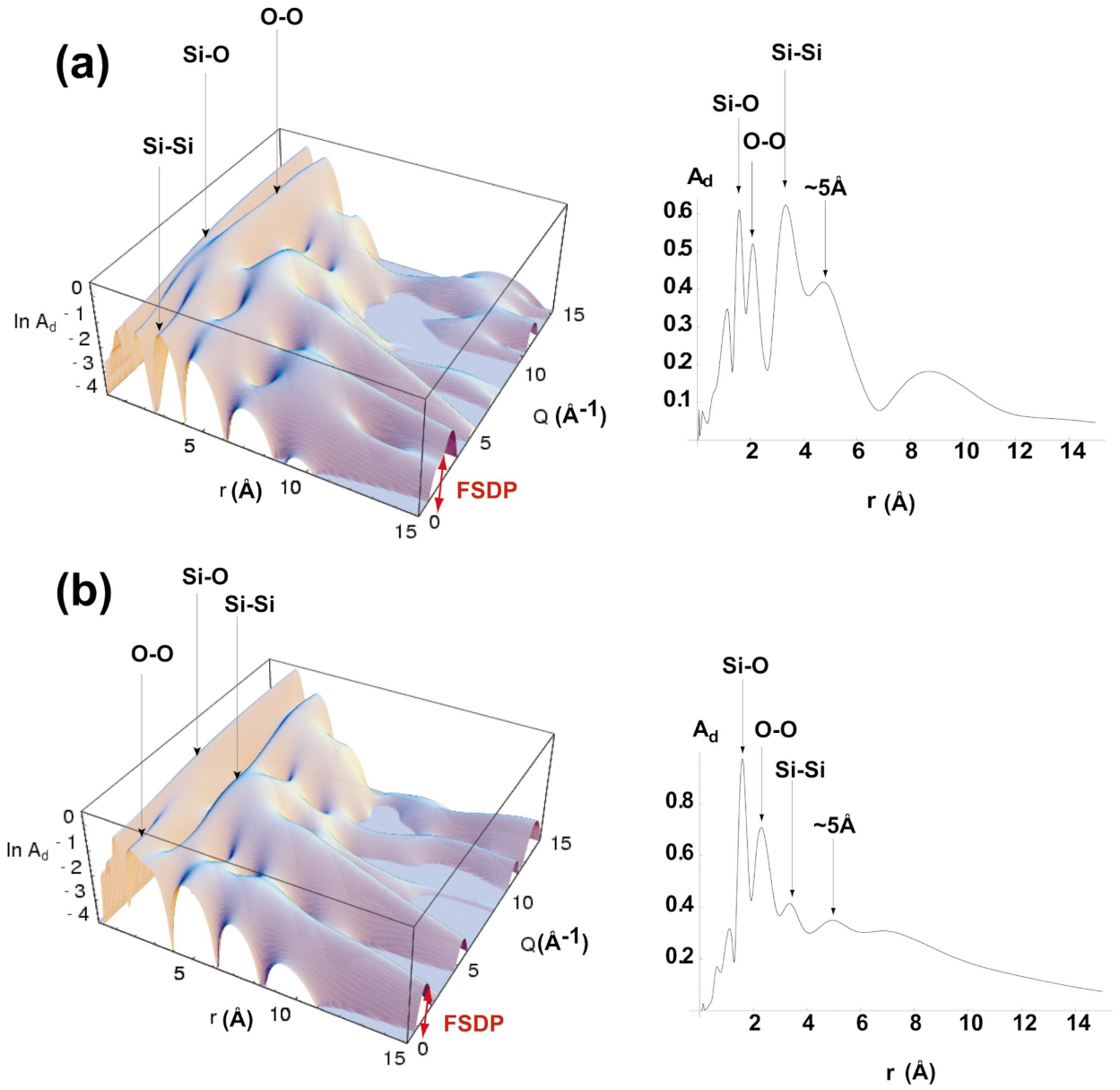

FIG. 1. (Color) Three-dimensional $r-Q$ diagrams of the instantaneous amplitude A_d of the CWT of the reduced (a) neutron and (b) x-ray experimental structure factors for silica glass. Short-range Si—O, O—O, and Si—Si correlations, along with the positions of the FDSP, are indicated by arrows. Cross sections of the CWT at 1.5 $Å^{-1}$ are also shown on the right-hand side of each wavelet diagram.

x-ray[19] diffraction data [see Figs. 1(a) and 1(b), respectively] using the wavelet technique. Since the details of the numerical procedures were given in our previous paper,[15] we here present a brief outline of the technique.

The basis set of the CWT contains localized oscillations characterized by two transform parameters, namely the scale (or dilation) and the translation. This makes the CWT more preferable, as compared with the Fourier transform, for the analysis of signals which contain rapidly varying frequencies and amplitudes, as mentioned earlier. In this work, the CWT is performed by calculating the set of inner products of $Q[S(|Q|)-1]$ with a basis set of wavelets $\Psi(t;\sigma)$. The functional form of the wavelet used in this work is as follows:[15]

$$\Psi(t;\sigma) = \pi^{-1/4} e^{-(1/2)t^2} \{p(\sigma)[\cos(\sigma t) - \kappa(\sigma)] + iq(\sigma)\sin(\sigma t)\},$$

where $p(\sigma)$ and $q(\sigma)$ are given by

$$p(\sigma) = (1 + 3e^{-\sigma^2} - 4e^{-(3/4)\sigma^2})^{-1/2}, \quad q(\sigma) = (1 - e^{-\sigma^2})^{-1/2},$$

with $\kappa(\sigma) = e^{-\sigma^2/2}$. This wavelet function has a tuning parameter, σ, which controls the number of oscillations in the envelope. This parameter has to be carefully chosen, since it allows "time and frequency" uncertainties to be traded. Smaller (larger) values of σ result in higher (poorer) resolution in Q space but poorer (higher) resolution in r space. We found that using $\sigma=7$ allows the best trade-off between

r-space and *Q*-space resolution in this case. It should be noted, however, that it is for smaller values of σ ($\leqslant 2$) that our new wavelet is markedly superior to, say, the Morlet wavelet. We then obtained the instantaneous amplitude, A_d, of a signal component using the stationary-phase approximation, as described in Ref. 15.

III. RESULTS

First, we concentrate our interest on the CWT diagrams in the distance range 1–3 Å, which characterizes the nearest-neighbor bonding environments of the cation-centered tetrahedral SiO_4 units. We see from Figs. 1(a) and 1(b) that, in this distance range, there exist three main ridges that are delocalized over a wide range of *Q* values in the CWT diagram. The peak positions of these ridges are located at ~1.6, ~2.6, and ~3.0 Å, which are in accordance with the reported nearest-neighbor Si—O (1.61–1.62 Å), O—O (2.62–2.64 Å), and Si—Si (3.06–3.07 Å) correlations in silica glass.[17] The interpretation of such ridges is that broad ranges of *Q* values in the structure factor are associated with particular short-range-order distances corresponding to the ridge peak positions. This demonstrates that the present CWT procedure reveals the short-range atom-atom correlations associated with the constituent SiO_4 tetrahedral units.

We next turn to the distance region beyond 3 Å in the CWT diagrams. In this region, in contrast to that below 3 Å, the CWT features appear as ridges delocalized in *r* space, but localized at particular *Q* values. It should also be noted that, in both Figs. 1(a) and 1(b), a ridge exists along the *r*-axis centered at a *Q* value of ~1.5 $Å^{-1}$, in agreement with the position of the FSDP in the corresponding structure factor. The ridge at $Q \sim 1.5$ $Å^{-1}$ is not uniformly delocalized over the entire *r* range, but decays almost exponentially for distances greater than ~10 Å. Thus a wide range of interatomic distances contribute to the formation of the isolated peak in *S*(*Q*) that is the FSDP. One can also see from Figs. 1(a) and 1(b) that the FSDP ridge at $Q \sim 1.5$ $Å^{-1}$ exhibits a broad, but strong, maximum at ~5 Å, before the rapid decay at longer distances. It should be noted, however, that the decay feature at longer distances ($r \gtrsim 7$ Å) depends strongly on the scattered sources, namely, neutrons and x rays although both the neutron and x-ray *S*(*Q*) data yield the same peak position of the respective FSDPs. This implies that the longer-distance ($r \gtrsim 7$ Å) structural correlations only have a minor influence on the position of the FSDP. Thus the present CWT analysis demonstrates that the dominant interatomic distance relevant to the FSDP is ~5 Å. This is basically in harmony with a previous finding that the shape of the FSDP in v-SiO_2 is especially sensitive to spatial correlations between 4 and 8 Å,[17] and that structural correlations for a distance greater than ~10 Å are of little importance.[7,20]

IV. DISCUSSION

The CWT diagrams have shown that dominant interatomic distance linked to the FSDP in silica glass is ~5 Å. It is hence interesting to investigate how interatomic correlations at ~5 Å in the random network of silica glass can create the low-*Q* feature in *S*(*Q*), the FSDP. Figure 2 shows a schematic view of a series of atom-centered spheres with a radius of ~5 Å. Each shell of the spheres, along with their centers, is characterized by a high density of atoms of interest. In a glass network, these spheres and their centers are not arranged so as to form regular planes of atoms on a long-range length scale. However, if we concentrate on the length scale of ~5 Å, a set of three contiguous "planes" of high atomic density, which consist of atoms in centers and shells of two adjacent spheres, is well defined, irrespective of the random nature of the network (see Fig. 2). In other words, two adjacent spheres are likely to create such a set of local "planes" of high atomic density on the medium-range length scale. According to previous classical[17,21,22] and *ab initio*[23] molecular-dynamics (MD) simulations of silica glass, a peak at ~5 Å in the real-space atomic-density correlation functions results from second-nearest-neighbor Si—Si and O—O separations, i.e., Si—O—Si—O—Si and O—Si—O—Si—O correlations. This implies that both Si and O atoms will contribute to the formation of a set of planes of high atomic density. Indeed, as shown in Fig. 3, such sets of parallel local planes can be identified in model silica glass networks, which have been created by *N*-*P*-*T* -MD simulations using 1500 atoms with a modified potential[24] originally proposed by van Beest *et al.*[25] and by quenching from the melt ($T = 6000$ K) to the well-relaxed glassy state ($T \sim 10^{-4}$ K) at an average quench rate of ~1 K/ps. In our previous paper,[26] we showed that the model glass thus created has reproduced fundamental structural and vibrational properties of actual silica glass. We see from Fig. 3 that these sets of planes are decorated by both Si and O atoms, and, in between the planes, there is a region of low atomic density (or "voids"[6]). Thus the second-neighbor Si—Si and O—O correlations at ~5 Å occur in such a coherent manner as to form a set of near-parallel local "planes" of high atomic density, whose (medium-range) length scale is comparable with that of the interatomic correlations of ~5 Å. It is expected that interatomic correlations

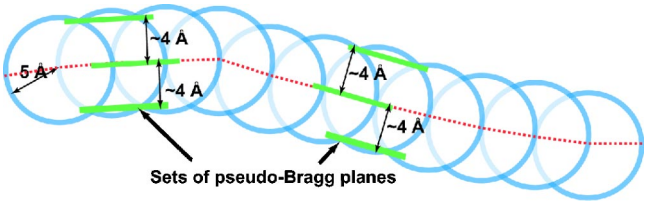

FIG. 2. (Color online) A schematic representation of the formation of pseudo-Bragg planes as a result of atom-atom correlations at ~5 Å. The circles indicate atom-centered spheres of high atomic density resulting from second-nearest-neighbor Si—Si (or O—O) separations. Centers of the spheres are linked by a dotted line. This dotted line is not straight but winding because of the random nature of the glass network. Even in such a random network, a set of three contiguous near-parallel planes of high atomic density (see the bold lines), whose length scale is comparable to the radius of the spheres (~5 Å), can be well defined. In real silica glass, it is expected that these planes will be decorated by both Si and O atoms. The resulting interplanar distance is less than ~5 Å; a probable value is ~4 Å because of geometrical considerations.

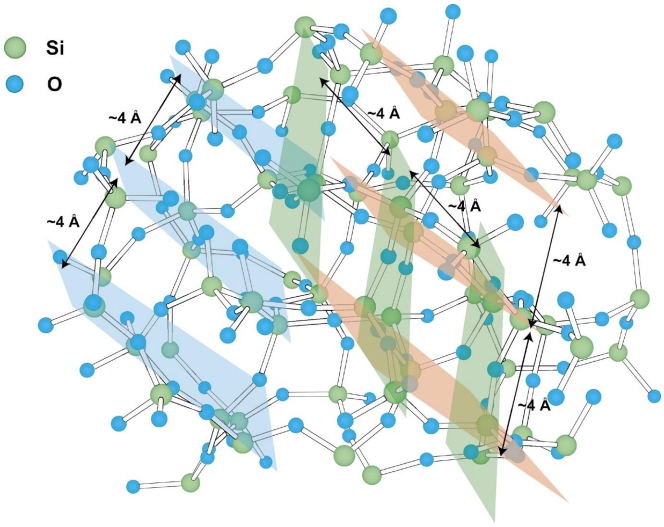

FIG. 3. (Color) A moiety of a simulated model of silica glass obtained from classical MD calculations showing the identification of several sets of parallel local planes decorated by Si and O atoms. These sets of planes can be found practically everywhere in the simulated silica glass. The interplanar separation is ~4 Å, whereas the major Si—Si and O—O interatomic separations between the planes are ~5 Å, accounting for the peak at ~5 Å seen in the cross sections of the CWT at $Q_{\mathrm{FSDP}}=1.5$ Å^{-1} ($2\pi/Q_{\mathrm{FSDP}}=\sim 4$ Å) in Fig. 1.

at larger distances (see, for example, a weak maximum at −7.5 Å in the WT diagrams) also contribute to the formation of such local planelike configurations, but the coherence of such contributions will decrease with increasing distance. It is also worth mentioning that, from the geometrical considerations shown in Fig. 2, the perpendicular (noninteratomic) distance between the parallel planes, or "periodicity," is ~4 Å. A similar correlation distance has been found in the model glass network as well in the distance range from 4.0 to 4.2 Å (see also Fig. 3). That is, as far as the medium-range length scale is concerned, local "pseudo-Bragg" planes having an interplanar spacing of ~4 Å can be defined, even in the glassy SiO_2 network. However, the spatial extent of these local quasi-Bragg planes is insufficient to give rise to appreciable anisotropy in the $\boldsymbol{k}$-vector-dependent structure factor $A(\boldsymbol{k})$, which has been used as a monitor for extensive layering in disordered structures.[8] It is hence reasonable to assume that these planes, which are defined only on the medium-range length scale, are responsible for much of the constructive diffraction leading to the FSDP in $S(Q)$, in the case of silica glass characterized by a "period" of $2\pi/Q_{\mathrm{FSDP}}\cong 4.1$ Å. Of course, the density fluctuations associated with the "pseudo-Bragg" planes tend to vanish over a length scale of 10–15 Å because of local disorder, especially in dihedral angles, leading to a more random nature of the glass network on longer-range length scales, thereby explaining the rapid spatial decay of the FSDP ridge at $Q\sim 1.5$ Å^{-1} in the CWT for distances greater than 10 Å.

Finally, we should note that our structural model for the origin of the FSDP is not identical to a previous quasilattice plane model,[7] which assumes crystallinelike layers in the glass structure. Our model does not necessarily require a crystalline counterpart to account for the FSDP, although the position of the FSDP for silica glass does correspond closely to that of the Bragg-diffraction peak from {101} planes of α-cristobalite. It may be true that structural arrangements similar to those found in α-cristobalite are, in part, responsible for the "pseudo-Bragg" planes in silica glass, but this does not mean that crystallinelike layered structures exist in the glassy system. In the present picture, these planes of high atomic density result from collective structural correlations among second- and third-neighbor SiO_4 structural units in the SiO_2 network and the resultant r-space ordering at ~5 Å.

V. CONCLUSIONS

We have shown that the present approach, combining "time-frequency" continuous wavelet transform analysis with molecular-dynamics simulations, enables us to predict the nature of medium-range structural ordering in silica glass. Interatomic distances in the region of $r\sim 5$ Å, associated with a couple of local "pseudo-Bragg" planes, are a manifestation of medium-range order in silica glass. Whether or not the structural ordering pertaining to local planes, which we have found in structural models of silica glass, is present in other glassy systems, and hence can give a unified picture of the FSDP in glasses, remains to be seen. However, we believe that our method of time-frequency wavelet analysis, which we refer to as "real-reciprocal space analysis," is uniquely able to clarify this issue.

ACKNOWLEDGMENT

We thank M. Arai and S. Kohara for providing us with neutron and x-ray scattering data, respectively, on silica glass.

[1] S. R. Elliott, *Physics of Amorphous Materials*, 2nd ed. (Longman, London, 1990).
[2] S. R. Elliott, Nature (London) **354**, 445 (1991).
[3] P. H. Gaskell, J. Non-Cryst. Solids **293–295**, 146 (2001).
[4] J. D. Martin, S. J. Goettller, N. Fossé, and L. Iton, Nature (London) **419**, 381 (2003).
[5] W. A. Crichton, Nature (London) **414**, 622 (2001).
[6] S. R. Elliott, Phys. Rev. Lett. **67**, 711 (1991).
[7] P. H. Gaskell and D. J. Wallis, Phys. Rev. Lett. **76**, 66 (1996).
[8] C. Massobrio and A. Pasquarello, J. Chem. Phys. **114**, 7976 (2001).
[9] A. C. Wright, R. A. Hulme, D. Grimley, R. N. Sinclair, S. W. Martin, D. L. Price, and F. L. Galeener, J. Non-Cryst. Solids **129**, 213 (1991).
[10] J. van den Berg, *Wavelets in Physics* (Cambridge University Press, Cambridge, England, 1999).

[11] C. Torrence and G. P. Compo, Bull. Am. Meteorol. Soc. **79**, 61 (1998).
[12] D. B. Percival and A. T. Walden, *Wavelet Methods for Time Series Analysis* (Cambridge University Press, Cambridge, England, 2000).
[13] I. Daubechies, *Ten Lectures on Wavelets* (Society of Industrial and Applied Mathematics, Philadelphia, 1992).
[14] Y. Ding, T. Nanba, and Y. Miura, Phys. Rev. B **58**, 14 279 (1998).
[15] J. D. Harrop, S. N. Taraskin, and S. R. Elliott, Phys. Rev. E **66**, 026703 (2002); **68**, 019904 (2003).
[16] P. Goupillaud, A. Grossmann, and J. Morlet, Geoexploration **23**, 85 (1984).
[17] P. Vashishta, R. K. Kalia, J. P. Rino, and J. Ebbsjo, Phys. Rev. B **41**, 12 197 (1990).
[18] Y. Inamura, M. Arai, M. Nakamura, T. Otomo, N. Kitamura, S. B. Bennington, A. C. Hannon, and U. Buchenau, J. Non-Cryst. Solids **293–295**, 389 (2001).
[19] S. Kohara, K. Suzuya, Y. Kashihara, N. Matsumoto, N. Umesaki, and I. Sakai, Nucl. Instrum. Methods Phys. Res. A **467–468**, 1030 (2001).
[20] P. S. Salmon, Proc. R. Soc. London, Ser. A **445**, 351 (1994).
[21] J. P. Rino, I. Ebbsjö, R. K. Kalia, A. Nakano, and P. Vashishta., Phys. Rev. B **47**, 3053 (1993).
[22] S. N. Taraskin and S. R. Elliott, Phys. Rev. B **56**, 8605 (1997).
[23] J. Sarnthein, A. Pasquarello, and R. Car, Phys. Rev. B **52**, 12 690 (1995).
[24] Y. Guissani and B. Guillot, J. Chem. Phys. **104**, 7633 (1996).
[25] B. W. H. van Beest, G. J. Kramer, and R. A. van Santen, Phys. Rev. Lett. **64**, 1955 (1990).
[26] S. N. Taraskin and S. R. Elliott, Phys. Rev. B **59**, 8572 (1999).